Comparison of adaptive mono-component decompositions

Tao Qian [a], Hong Li [b,*], Michael Stessin [c]

[a] *Department of Mathematics, Faculty of Science and Technology, University of Macau, Taipa, Macao, China*
[b] *School of Mathematics and Statistics, Huazhong University of Science and Technology, Wuhan 430074, China*
[c] *Department of Mathematics and Statistics, University of Albany (SUNY), NY 12222, United States*

ARTICLE INFO

ABSTRACT

As presented in some recent publications, adaptively choosing the parameters of a Takenaka–Malmquist (TM) system according to the given signal gives rise to the so called adaptive Fourier decomposition (AFD). Besides optimal selections of the parameters to ensure the maximal energy gain at each step, AFD produces entries of non-negative analytic instantaneous frequency. The latter enables us to define a reasonable time–frequency distribution with most desired properties. The energy principle together with the unwinding process through factorizing out the inner function factors yields two variations of the standard AFD, both having appeared in the literature. They are referred by this paper as, respectively, unwinding adaptive Fourier decomposition (UAFD) and double sequence unwinding adaptive Fourier decomposition (DSUAFD). After a short summary of the three adaptive decompositions, the present paper makes comparison between them, as well as with the traditional Fourier series decomposition (FD). The related Dirac type time–frequency distributions associated with mono-components and mono-component decompositions of multi-components are introduced with examples. As necessary preparation we recall the concept mono-component and related knowledge in the introduction section.

© 2012 Elsevier Ltd. All rights reserved.

1. Introduction

The analytic and rational functions

$$B_n(z) = B_{\{a_1, a_2, \ldots, a_n\}}(z) = \frac{\sqrt{1 - |a_n|^2}}{1 - \bar{a}_n z} \prod_{k=1}^{n-1} \frac{z - a_k}{1 - \bar{a}_k z}, \quad n = 1, 2, \ldots, \tag{1}$$

are known as an orthogonal rational function system or Takenaka–Malmquist system (TM system) that depends on a sequence of complex parameters $\{a_k\}$ in the unit disc $\mathbb{D}$. An entry B_n is called a modified Blaschke product. A TM system is a generalization of the Fourier system $\{z^n\}_{n=0}^{\infty}$ that corresponds to $a_k = 0$ for all k. The Laguerre basis and the two-parameter Kautz basis are also particular cases of the system (1). We will be working with the Hardy space $H^2(\mathbb{D})$. Denote the non-tangential boundary limits of the functions in $H^2(\mathbb{D})$ by $H_b^2(\partial\mathbb{D})$ that is a closed subspace of $L^2(\partial\mathbb{D})$. The mapping that maps functions in $H^2(\mathbb{D})$ to their non-tangential boundary limits (functions) in $H_b^2(\partial\mathbb{D})$ is an isometric isomorphism. The Hilbert space $H_b^2(\partial\mathbb{D})$ consists of the so called analytic signals, or physically realizable signals, that are identical with the

* Corresponding author. Tel.: +86 13618663109; fax: +86 27 87543231.
 E-mail addresses: fsttq@umac.mo (T. Qian), hongli@hust.edu.cn (H. Li), stessin@math.albany.edu (M. Stessin).

signals of finite energy whose Fourier series expansion only spans by the non-negative powers of the complex trigonometric function e^{it}. The inner product that we have for $L^2(\partial\mathbb{D})$ is

$$\langle F, G \rangle = \frac{1}{2\pi} \int_0^{2\pi} F(e^{it})\overline{G}(e^{it})dt.$$

Under the given inner product restrictions of the functions in (1) constitute an orthonormal system. As is well known, the condition

$$\sum_{k=1}^{\infty}(1 - |a_k|) = \infty \tag{2}$$

is sufficient and necessary for the associated orthonormal system $\{B_n(e^{it})\}$ to be a complete basis in the Hardy space $H_b^2(\partial\mathbb{D})$. The last mentioned sufficient and necessary condition can be extended to all $H_b^p(\partial\mathbb{D})$, $1 < p < \infty$. A complex-valued signal s is called a *complex mono-component* if it is the boundary limit of an analytic signal, and, under the amplitude–phase representation $s(t) = \rho(t)e^{i\theta(t)}$, it possesses the property $\theta'(t) \geq 0$, a.e. Note that the classical derivatives $\theta'(t)$ may not exist [1–5]. The notion of $\theta'(t)$ should be suitably defined, and be a generalization of the classical derivative. We define it in various cases through Hardy space decomposition [2,6]. For a complex mono-component $s(t) = \rho(t)e^{i\theta(t)}$ its *instantaneous frequency function* (IF function) is defined to be $\theta'(t)$. We call a real-valued signal s a *real mono-component* if $s + iHs$ is a complex mono-component, where H is the Hilbert transform of the context. The *instantaneous frequency* of a real mono-component s is defined to be the IF of the complex mono-component $s + iHs$. Both complex and real mono-components are abbreviated as mono-components that causes no confusion. Mono-components are generalizations of e^{int}, the latter being the boundary values of the monomials z^n. A complex-valued signal s is called a *pre-mono-component* if there exists $M > 0$ such that $e^{iMt}s(t)$ is a mono-component. Among boundary limits of functions in the Hardy space a large class of mono-components have been identified, including boundary values of Möbius transforms, Blaschke products of finite and infinite orders [7], starlike and p-starlike functions, modified Blaschke products [8,9], etc.

The referred studies [8,9], in particular, are among the new phase of the study of the Bedrosian identity [10] $H(fg) = fHg$, where H is the Hilbert transformation. This new phase of study aimed to assert at what conditions the quadrature form $\rho(t)e^{i\theta(t)}$ is again a mono-component if $e^{i\theta(t)}$ is assumed to be a mono-component. It is essentially the main results of [8,9] that if the phase signal $e^{i\theta(t)}$ is from a Blaschke product of $n - 1$ zeros, then the desired mono-component $\rho(t)e^{i\theta(t)}$ is intimately related to modified Blaschke products B_n. In a TM system each modified Blaschke product B_n, being restricted to the boundary, is an analytic signal, and is either a mono-component or pre-mono-component for $M = 1$. If one of the parameters $a_1, \ldots, a_{n-1}$ in relation to B_n is identical with 0, then z is a factor of B_n, and B_n is a mono-component.

A decomposition into a sum of mono-components is called a *mono-component decomposition* [7]. A given signal can have more than one mono-component decompositions among which Fourier series is a particular one. The interesting ones are those of a fixed type of mono-components with increasing phase derivatives in the sequel, and of fast convergence. The most popular and important type of mono-components would be the rational mono- or pre-mono-components in the TM system, viz. the modified Blaschke products. In terms of fast convergence in energy we raise the concept *adaptive mono-component decomposition* (AMD) [1,2,7,11].

All traditional studies of the TM system are based on a prescribed sequence of parameters $a_1, \ldots, a_n, \ldots$ satisfying the condition (2). In [12], instead of using a prescribed sequence $\{a_k\}$ we consecutively select $\{a_k\}$ according to the given signal f to be decomposed. The selections of a_k's are based on the energy principle: at each selection of a new parameter we can achieve the maximal energy gain. The algorithm thus achieves fast convergence in energy. Fast convergence of AFD decomposition, in both the energy and the pointwise sense are verified by experiments. By combining the AFD algorithm with the factorization mechanism in view of minimum energy delay property of outer functions we propose an unwinding adaptive Fourier decomposition (UAFD) in [11] (see Section 3). In the most recent paper [13] we propose a third adaptive mono-component decomposition that, besides the unwinding process, incorporates an optimal selection of a pair of two parameters at each step, corresponding to two infinite series at the end, called DSUAFD. The facts that UAFD and, especially, DSUAFD belong to the mono-component decomposition rest on the newly proved theoretical result on positivity of phase derivatives of boundary limits of inner functions [7]. In the present paper we will recall and compare the formulations and effectiveness of the three newly established AMD methods, and discuss their ideas and merits. Some comparisons between them are based on numerical examples.

The types of new function decompositions are intended to treat the so called transient signals. A precise definition of transient signal involves the stochastic process. In other words, transient signals are random signals. They are usually nonlinear and non-stationary. To study such signals the concept instantaneous frequency (IF) cannot be avoided, and the IFs are preferably non-constant, such as those for nonlinear Fourier atoms [14]. It is well known that the traditional Fourier decomposition can only provide the total amount of each frequency in the whole time range. This disadvantage is due to the linear-phase-representation of Fourier in terms of trigonometric functions, or Fourier atoms, which are of linear phase. It, in particular, cannot tell at a certain time moment, what types of frequencies present and what are their respective amounts. In all the three proposed decomposition methods there exist well defined IFs. The reason we name them in relation to Fourier is that they are directly related to analytic and harmonic function theory. It is this characterization that distinguishes themselves from wavelets, short time/window Fourier, or Gabor transform, etc.

Although being modest ones, there do exist convergence rate estimates proved for AFD and, in general, for greedy algorithm [15]. There are also recent studies that show that for TM bases there exist the same pointwise convergence results and convergence rate estimates as for the Fourier series case [16–19]. The reason we prefer the new types of decomposition methods to the traditional ones is again for the course of transient signals. Indeed, a transient signal $s(\zeta, t)$ can be the trace of a Brownian motion at a probability state ζ that does not possess any smoothness. Therefore, seeking for convergence rate estimates under smoothness conditions for the AFD type decompositions is not a right direction. On the other hand, to treat transient signals, adaptive approximation by the TM system through parameter selection to get maximal energy gain from each remainder and factorization in view of the energy delay seem to be among sensible strategies.

TM bases have long been interested with applications in various engineering practices, especially in physics (optics), control theory, and, in particular, in system identification. One cannot exhaust the relevant literature but can mention [16–18,20–25]. Most recently Pap extended the concept of wavelets to TM bases in which the poles defining the TM basis satisfy some group relations [26]. The mentioned studies, however, aim to treat TM bases. In other words, they are based on prescribed parameters a_k's satisfying the hyperbolic non-separable condition (2). In those studies the non-negative phase derivative aspect of TM bases and its applications to signal analysis are not explored. TM systems that are not necessarily bases, on the other hand, are related to Beurling's and Beurling–Lax's Theorems, and especially, shift- and backward shift- invariant subspaces of the Hardy spaces. AFD, because of its selection of poles, can be classified into the category of general TM systems other than bases. Like the traditional TM basis decompositions, AFD has found its applications in system identification [12,27,28]. Based on AFD a practical algorithm of the best approximation to signals in the Hardy H^2 space by rational functions of degree less than a prescribed positive integer n was recently proposed in [29]. If a system is given by an ordinary differential equation, through Laplace transformation the solution is reduced to solving a Laplace-multiplier problem of rational function type. This observation indicates that TM bases and TM systems are naturally related to rational function approximation problems. To conclude, there is a great potential for applications of the three introduced AFD related decompositions. As a matter of fact, whenever a practical problem can be treated by the traditional Fourier series decomposition (FD), then it can also be treated by using AFD, or UAFD, or DSUAFD. Related interest can be found in [30,31]. In this paper, for completeness of the story, we introduce, and provide examples for, the Dirac type time–frequency distributions of mono-components and multi-components. The Dirac type distributions follow Cohen [32] and are first studied in the Ph.D. Thesis of Dang Pei at University of Macau.

This paper concentrates in periodic or discrete physically realizable signals corresponding to $H^2(\mathbb{D})$. For physically realizable signals in the whole time range, i.e. those in $H^2(\mathbb{C}^+)$, there is a parallel theory. Decompositions of real-valued signals in the $L^2(\mathbb{R})$-space can be obtained through the decompositions of their Hardy space projections. In the real-$L^2(\partial\mathbb{D})$ signal case, for instance, we have $s = 2[\text{Re}s^+] - c_0$, where $s^+ = \frac{1}{2}(s + iHs)$, and c_0 is the 0-th Fourier coefficient of s (see [12]).

In Sections 2–4 we review, respectively, AFD, UAFD and DSUAFD. Section 5 introduces the mono-component based time–frequency distributions (MTFDs) for mono-components and multi-components. Section 6 devotes to numerical experiments together with analysis on the merits of the individual algorithms.

2. AFD

Let $f \in H^2(\mathbb{D})$. To expand f into its Fourier series we successively project $f = f_1$ and the reduced remainders $f_n(z) = r_n(z)/z^n$ onto the unit vector 1, where r_n denotes the standard remainder defined as the difference between f and the n-th partial sum. In AFD, instead of projecting f_1 onto the unit vector 1, we project it onto the *normalized reproducing kernel*

$$e_{\{a\}}(z) = \frac{\sqrt{1 - |a|^2}}{1 - \bar{a}z}, \quad a \in \mathbb{D}.$$

Note that $e_{\{a\}}$ is a generalization of 1 due to $e_{\{0\}} = 1$. In the terminology of greedy algorithm the related dictionary is

$$\mathcal{D} := \left\{ e_a(z) = \frac{\sqrt{1 - |a|^2}}{1 - \bar{a}z}, \ a \in \mathbb{D} \right\}, \tag{3}$$

where $\mathbb{D}$ denotes the open unit disc in the complex plane $\mathbb{C}$. By using Cauchy's integral formula, we have

$$\langle f_1, e_{\{a\}} \rangle = \sqrt{1 - |a|^2} f_1(a).$$

The first step is the adaptive selection of $a = a_1 \in \mathbb{D}$ such that

$$|\langle f_1, e_{\{a_1\}} \rangle|^2 = (1 - |a_1|^2)|f_1(a_1)|^2 = \max\{(1 - |a|^2)|f_1(a)|^2 : a \in \mathbb{D}\}.$$

In [12] we prove that such optimal a_1 is attainable at a point in $\mathbb{D}$ for any function $f_1 \in H^2(\mathbb{D})$. This result is called the *Maximal Energy Principle*. The standard remainder

$$r_1(z) = f_1(z) - \sqrt{1 - |a|^2} f_1(a_1)$$

is accordingly minimized. We next find the reduced remainder f_2 by

$$r_1(z) = f_2(z) \frac{z - a_1}{1 - \overline{a}_1 z}. \tag{4}$$

Note that r_1 has zero a_1, and thus f_2 is in $H^2(\mathbb{D})$. In general, the recursive formula to obtain f_{k+1} from f_k is the a_k-*backward shift* of f_k:

$$f_{k+1}(z) = \frac{f_k(z) - \langle f_k, e_{\{a_k\}} \rangle e_{\{a_k\}}(z)}{\frac{z - a_k}{1 - \overline{a}_k z}}, \tag{5}$$

where

$$a_k = \arg\max\{ |\langle f_k, e_{\{a\}} \rangle| : a \in \mathbb{D} \}.$$

In terms of the standard remainder we have

$$r_n(z) = f_{n+1}(z) \prod_{k=1}^{n} \frac{z - a_k}{1 - \overline{a}_k z}. \tag{6}$$

We call such a process from f_k to f_{k+1} through finding a maximizer a_k for

$$|\langle f_k, e_{\{a\}} \rangle| = \sqrt{1 - |a|^2} |f_k(a)|$$

a *maximum sift*. If a_k does not give rise to the maximum, we can still carry on the process, then we call the process just a *sift*, or a *sift through* a_k. Möbius factors are accumulated and form finite order Blaschke products. The entry that we obtain at the n-th sift is $\langle f_n, e_{\{a_n\}} \rangle B_n(z)$. If all the sifts are maximum sifts, then the corresponding decomposition is an AFD. Indeed, under maximum sifts we can show [12]

$$f = \sum_{k=1}^{\infty} \langle f_k, e_{\{a_k\}} \rangle B_k = \sum_{k=1}^{\infty} \langle f, B_k \rangle B_k,$$

although the selected a_k's do not necessarily satisfy the condition (2).

Note that a-backward shift is a generalization of the ordinary backward shift operator. Indeed, the case $a = 0$ corresponds to the latter. It is interesting to know that the recursive formula is just the generalized backward shift.

AFD is considered to be a realizable variation of greedy algorithm [15,33,34]. It is realizable, for at each selection we can, theoretically, get the maximum energy gain; and it is a variation because the optimal selection for the parameter at each step is not for the standard remainder, but for the reduced remainder. More aspects of the algorithm of AFD are studied in [35]. AFD has been used to practical problems including system identification and speech analysis [27].

3. Unwinding AFD

Unwinding AFD was motivated by the following observation in digital signal processing. Let $X(z)$ and $Y(z)$ be the Z-transforms of, respectively, the physically realizable signals $x = (x_0, x_1, \ldots, x_n, \ldots)$ and $y = (y_0, y_1, \ldots, y_n, \ldots)$. Assume there exists the relation $Y = GX$, where G is an inner function. By definition an inner function in the unit disc is a bounded analytic function whose non-tangential boundary limits are of unit module almost everywhere on the unit circle. Due to the unimodular property of G, there follows

$$\|X\| = \|Y\|.$$

The Plancherel Theorem gives

$$\sum_{k=0}^{\infty} |x_k|^2 = \sum_{k=0}^{\infty} |y_k|^2.$$

One can show, however, for any integer $N \geq 0$,

$$\sum_{k=0}^{N} |x_k|^2 \geq \sum_{k=0}^{N} |y_k|^2$$

(see [6,36]). This amounts to say that all-pass filters cause "energy delay". One can further show that if the equal sign holds for a particular pair of signals x and y, then G must be of the form

$$G(Z) = \frac{y_0 + y_1 Z + \cdots + y_N Z^N}{x_0 + x_1 Z + \cdots + x_N Z^N}, \tag{7}$$

where the denominator of $G(Z)$ has no zero in or on the unit circle [6,36]. This implies that if G is not of such form, then the energy gain in the output signal Y is strictly delayed at each step. This suggests that in a mono-component decomposition, in order to get fast convergence, we should factorize out at each step the inner function factor and only decompose the outer function part.

This mechanism can also be explained as follows. Suppose one wishes to decompose a function that, by nature, only has higher frequencies, such as $f(z) = z^n g(z)$, where g is in $H^2(\mathbb{D})$. Thus in the Taylor series expansion of f the non-zero coefficients start from c_n. For such functions if one produces a mono-component decomposition starting from the very low degree in the TM system, then the process is mandatory, and convergence cannot be expected to be fast. The natural way is to first factorize out the inner function factor in the Nevanlinna factorization of the signal.

In the above example we should at least first factorize out the factor z^n. We call the factorization procedure *unwinding*.

The actual algorithm goes as follows. Let $f \in H^2(\mathbb{D})$, and $f = I_1 f_1$, where I_1 is the inner function factor of f in its Nevanlinna factorization, and f_1 is the outer function factor. The maximum sift process is applied to f_1 that results in

$$f(z) = I_1(z)[f_1(z) - \langle f_1, e_{\{a_1\}} \rangle e_{\{a_1\}}(z)] + I_1(z)\langle f_1, e_{\{a_1\}} \rangle e_{\{a_1\}}(z)$$
$$= I_1(z)g_1(z) + I_1(z)\langle f_1, e_{\{a_1\}} \rangle e_{\{a_1\}}(z).$$

Write

$$g_1(z) = h_2(z) \frac{z - a_1}{1 - \bar{a}_1 z}$$
$$= I_2(z) f_2(z) \frac{z - a_1}{1 - \bar{a}_1 z},$$

where I_2 and f_2 are the inner and outer factors of $h_2 \in H^2(\mathbb{D})$. Successively, we obtain

$$f(z) = \left(\prod_{i=1}^{n+1} I_i(z) \right) f_{n+1}(z) \left(\prod_{i=1}^{n} \frac{z - a_i}{1 - \bar{a}_i z} \right) + \sum_{j=1}^{n} \left(\prod_{i=1}^{j} I_i(z) \right) \langle f_j, e_{\{a_j\}} \rangle B_j(z),$$

where h_{n+1} is the a_n-backward shift of f_k,

$$h_{n+1}(z) = \frac{f_n(z) - \langle f_n, e_{\{a_n\}} \rangle e_{\{a_n\}}(z)}{\frac{z - a_n}{1 - \bar{a}_n z}}, \qquad (8)$$
$$h_{n+1} = I_{n+1} f_{n+1},$$

and the outer function f_{n+1} is given by

$$f_{n+1}(z) = e^{\frac{1}{2\pi} \int_0^{2\pi} \frac{e^{it} + z}{e^{it} - z} \log |h_{n+1}(e^{it})| dt}.$$

Next we use maximum sift to f_{n+1} and obtain a_{n+1}, and so on.

The last formula for finding the outer function in the Nevanlinna factorization is referred to any book of Hardy spaces (e.g., [37]), and

$$f(z) = \sum_{j=1}^{\infty} \left(\prod_{i=1}^{j} I_i(z) \right) \langle f_j, e_{\{a_j\}} \rangle B_j(z)$$

(see [11]).

4. Double sequence unwinding AFD

The DSUAFD algorithm is motivated by the same idea. The actual process involves selection of two parameters at one time, as given below [13].

$$f(z) = I_1(z) f_1(z)$$
$$= I_1(z) \left(f_1(z) - A_1 - \frac{B_1 z}{1 - \bar{a}_1 z} \right) + I_1(z) \left(A_1 + \frac{B_1 z}{1 - \bar{a}_1 z} \right),$$

where the role of A_1 is to make $f_1(z) - A_1$ have the zero 0, and $B_1 = B(f_1, A_1, a_1)$ is the constant that makes $\frac{B_1 z}{1 - \bar{a}_1 z}$ to be the projection of $f_1(z) - A_1$ onto $\frac{z}{1 - \bar{a}_1 z}$, where a_1 is chosen so that

$$\left\| f_1 - A_1 - \frac{B_1(\cdot)}{1 - \bar{a}_1(\cdot)} \right\| = \min \left\{ \left\| f_1 - A_1 - \frac{B(\cdot)}{1 - \bar{a}(\cdot)} \right\| : a \in \mathbb{D} \right\},$$

where $B = B(f_1, A_1, a)$, and $(\cdot)$ represents the variable z (see [13]). Recursively, we have a sequence of outer functions f_n and $d_n \geq 1$ such that

$$
\begin{aligned}
f(z) &= I_1(z)I_2(z)z \left(\frac{z - a_1}{1 - \bar{a}_1 z} \right)^{d_1} f_2(z) + I_1(z) \left(A_1 + \frac{B_1 z}{1 - \bar{a}_1 z} \right) \\
&= I_1(z)I_2(z)I_3(z)z^2 \left(\frac{z - a_1}{1 - \bar{a}_1 z} \right)^{d_1} \left(\frac{z - a_2}{1 - \bar{a}_2 z} \right)^{d_2} f_3(z) \\
&\quad + \left(A_2 + \frac{B_2 z}{1 - \bar{a}_2 z} \right) \left(\frac{z - a_1}{1 - \bar{a}_1 z} \right)^{d_1} I_1(z)I_2(z)z + I_1(z) \left(A_1 + \frac{B_1 z}{1 - \bar{a}_1 z} \right) \\
&= \cdots \\
&= \left(\prod_{i=1}^{n+1} I_i(z) \right) z^n \prod_{i=1}^{n} \left(\frac{z - a_i}{1 - \bar{a}_i z} \right)^{d_i} f_{n+1}(z) \sum_{j=1}^{n} \left(A_j + \frac{B_j z}{1 - \bar{a}_j z} \right) \left(\prod_{i=1}^{j} I_i(z) \right) z^{j-1} \prod_{i=1}^{j-1} \left(\frac{z - a_i}{1 - \bar{a}_i z} \right)^{d_i} \\
&= \sum_{j=1}^{\infty} \left(A_j + \frac{B_j z}{1 - \bar{a}_j z} \right) \left(\prod_{i=1}^{j} I_i(z) \right) z^{j-1} \prod_{i=1}^{j-1} \left(\frac{z - a_i}{1 - \bar{a}_i z} \right)^{d_i}.
\end{aligned}
$$

Note that the factors

$$
A_j + \frac{B_j z}{1 - \bar{a}_j z}
$$

are, in fact, with $A_j = f_j(0)$ and

$$
B_i = \begin{cases} O_i'(0), & \text{if } a_i = 0; \\ a_i^{-1}(1 - |a_i|^2)[O_i(a_i) - O_i(0)], & \text{if } a_i \neq 0. \end{cases} \qquad d_i = \begin{cases} 0, & \text{if } O_i'(0) = 0; \\ 1, & \text{if } a_i \neq 0. \end{cases}
$$

They generate two series, and that is the reason why it is called double sequence AFD. The role of the two sequences is to produce, besides UAFD, one extra factor z at each step so to ensure really faster convergence than Fourier series (see the proof in [13]). The first term A_j of the factor gives rise to a series whose entries are all inner functions. The second term $\frac{B_j z}{1 - \bar{a}_j z}$ corresponding to the maximum sift process gives rise to what we have in UAFD in relation to the TM system. We note that DSUAFD is always a mono-component decomposition due to existence of the powers of z in the entries.

5. MTFD

The *mono-component-based time–frequency distribution* (MTFD) of a mono-component signal $s(t) = \rho(t)e^{i\varphi(t)}$ is defined to be

$$
P(t, \xi) = \rho^2(t)\delta_M(\xi - \varphi'(t)), \quad (t, \xi) \in \mathbb{R} \times \left[-\frac{1}{2M}, +\infty \right) \tag{9}
$$

where

$$
\delta_M(\xi - \varphi'(t)) = \begin{cases} M & \text{if } \xi \in \left[\varphi'(t) - \frac{1}{2M}, \varphi'(t) + \frac{1}{2M} \right], \\ 0 & \text{if } \xi \notin \left[\varphi'(t) - \frac{1}{2M}, \varphi'(t) + \frac{1}{2M} \right]. \end{cases} \tag{10}
$$

There M is a large enough positive number. When $M = \infty$, then the L^2-function δ_M becomes the distributional Dirac (generalized) function. The reason for making M to be a finite number is for the mathematical convenience and practical applications.

If s is a multi-component in the Hardy space H^2, then through an adaptive mono-component decomposition s can be decomposed into a sum of mono-components

$$
s(t) = \sum_{k=1}^{\infty} s_k(t) \tag{11}
$$

or

$$
s(t) = \sum_{k=1}^{n} s_k(t) + r_n(t), \tag{12}
$$

Table 1
Relative energy errors of F_1.

Partial sum	DSUAFD	UAFD	AFD	FD
1	0.1910	0.1997	0.3294	0.1000×10^1
2	0.8203×10^{-1}	0.9880×10^{-1}	0.1444	0.1000×10^1
3	0.1121×10^{-1}	0.1037×10^{-1}	0.8033×10^{-1}	0.1000×10^1
4	0.3048×10^{-2}	0.3924×10^{-2}	0.4348×10^{-1}	0.9721
5	0.6439×10^{-3}	0.7141×10^{-3}	0.1388×10^{-1}	0.8640
6	0.1414×10^{-3}	0.1641×10^{-3}	0.9103×10^{-2}	0.7323
7	0.3652×10^{-4}	0.4548×10^{-4}	0.4039×10^{-2}	0.6082
8	0.7050×10^{-5}	0.7924×10^{-5}	0.2989×10^{-2}	0.5008
9	0.2132×10^{-5}	0.2646×10^{-5}	0.1502×10^{-2}	0.4110
10	0.3657×10^{-6}	0.3936×10^{-6}	0.1132×10^{-2}	0.3368

where r_n is the remainder in H^2. We note that adaptive mono-component decomposition is not unique. Under AFD, or UAFD, or DSUAFD the decomposing terms (11) are all mono-components (sometimes pre-mono-components). They are further orthogonal in those decompositions. Associated with every mono-component decomposition (11) or (12), an induced time–frequency distribution of s is defined, also called *mono-component-based time–frequency distribution* (MTFD), given by

$$P(t, \xi) = \sum_{k=1}^{\infty} P_k(t, \xi) = \sum_{k=1}^{\infty} \rho_k^2(t)\delta_M(\xi - \varphi_k'(t)), \quad (t, \xi) \in \mathbb{R} \times \left[-\frac{1}{2M}, \infty \right) \tag{13}$$

or

$$P(t, \xi) = \sum_{k=1}^{\infty} P_k(t, \xi) \approx \sum_{k=1}^{N} \rho_k^2(t)\delta_M(\xi - \varphi_k'(t)), \quad (t, \xi) \in \mathbb{R} \times \left[-\frac{1}{2M}, \infty \right), \tag{14}$$

where $P_k(t, \xi)$ is the MTFD of the mono-component s_k.

We can also induce an MTFD for a general signal s in L^2. To this end we first project s into the related Hardy space, that is to get s^+, then adaptively decompose s^+ into a sum of mono-components. Then we form the corresponding MTFD of s^+. The associated time–frequency distribution of s, called an MTFD of s, is defined to be identical with the MTFD of s^+.

MTFDs for mono- and multi-components have many desired properties for time–frequency distributions.

6. Comparison of four methods

In this section, comparisons of the four methods (DSUAFD, UAFD, AFD and FD) are made. Here the relative energy error of the Nth partial sum is defined as

$$E_1(f; n) = \frac{\|f - f_n\|^2}{\|f\|^2}, \tag{15}$$

where f_n is the n-th partial sum of the decomposition. In addition, we have the pointwise error

$$E_2(f; n) = \sum_{i=1}^{m} |f(i) - f_n(i)|, \tag{16}$$

where $f(i)$ and $f_n(i)$ are the i-th interpolating points of f and f_n, respectively. In our experiments, four functions were used. The experiments were conducted on a computer with 2 GB RAM and 2.66 GHz Intel Core 2 Duo processor and the code was implemented in MATLAB.

6.1. Experiment 1

The original signal (adopted from control theory) is

$$F_1 = \frac{0.0247z^4 + 0.0355z^3}{(1 - 0.9048z)(1 - 0.3679z)} \in H^2, \tag{17}$$

where $z \in \mathcal{C}$.

Figs. 1–5 show the real parts of the original signal and of the partial sums corresponding to the four algorithms. Tables 1 and 2 illustrate the relative energy errors and pointwise errors. The results of 10 iterations are given. If we decompose the signal 4 times, the relative energy errors of DSUAFD, UAFD, AFD, and FD are respectively 0.3048×10^{-2}, 0.3924×10^{-2}, 0.4348×10^{-1} and 0.9721. It is easy to find that DSUAFD has the best performance, and that of UAFD is close. In terms of iteration numbers, their approximations are obviously better than AFD and FD. As shown by the experiment, the
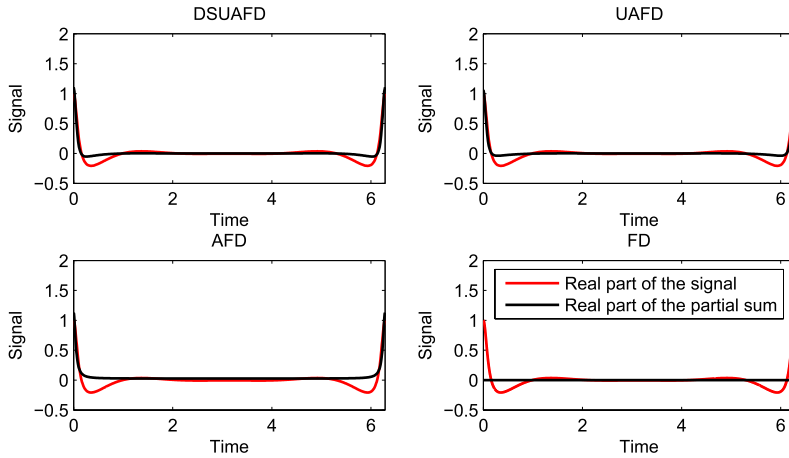
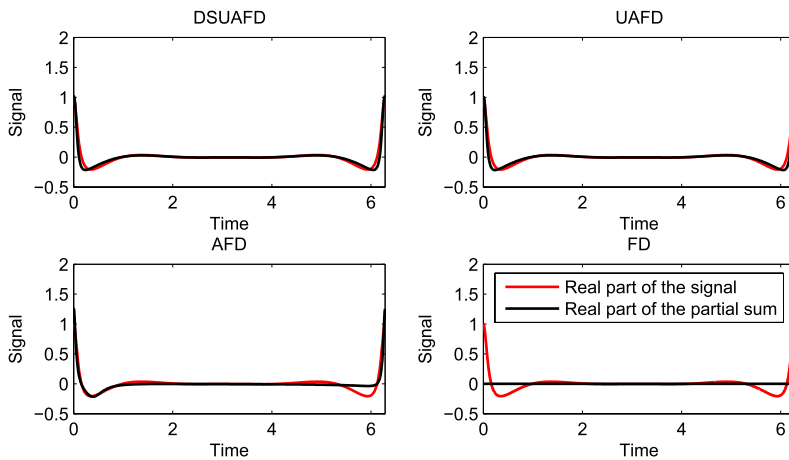**Fig. 1.** The 1st partial sums of F_1.

Fig. 2. The 2nd partial sums of F_1.

Table 2
Pointwise errors of F_1.

Partial sum	DSUAFD	UAFD	AFD	FD
1	0.1245×10^2	0.1259×10^2	0.1816×10^2	0.1391×10^2
2	0.5868×10^1	0.6229×10^1	0.1122×10^2	0.1391×10^2
3	0.2692×10^1	0.2604×10^1	0.1001×10^2	0.1391×10^2
4	0.1284×10^1	0.1411×10^1	0.5942×10^1	0.1582×10^2
5	0.6492	0.6651	0.4820×10^1	0.1587×10^2
6	0.2906	0.3084	0.3239×10^1	0.1492×10^2
7	0.1583	0.1705	0.2384×10^1	0.1380×10^2
8	0.6675×10^{-1}	0.6929×10^{-1}	0.2202×10^1	0.1256×10^2
9	0.3856×10^{-1}	0.4131×10^{-1}	0.1417×10^1	0.1134×10^2
10	0.1538×10^{-1}	0.1560×10^{-1}	0.1217×10^1	0.1034×10^2

approximation of AFD is significantly better than that of FD (see Table 1). The error curves are given in Fig. 6. The pointwise errors of DSUAFD, UAFD, and AFD exhibit a similar phenomena. Table 3 presents the comparison of the respective computer running times. (Note that N/A stands for "Not Applicable".) It shows that DSUAFD and UAFD require more running time than AFD and FD. This is no wonder, as the factorization process costs a lot of time. To reach the same error, the running time of AFD is less than that of FD. AFD involves much less iterations. The iteration numbers of DSUAFD, UAFD, AFD and FD are, respectively, 7, 7, 22 and 55, when the error tolerance is 0.5×10^{-4}.
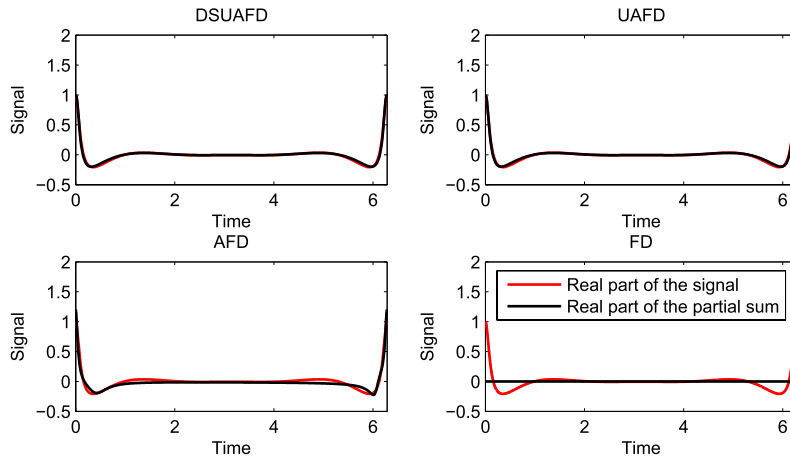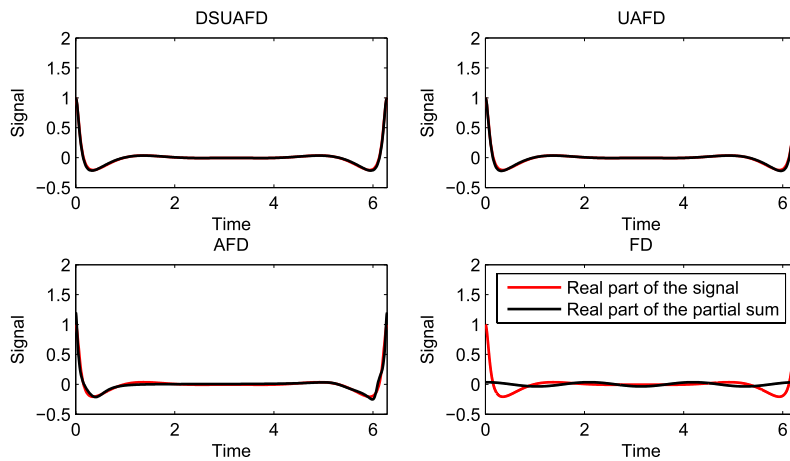
Fig. 3. The 3rd partial sums of F_1.

Fig. 4. The 4th partial sums of F_1.

Table 3
Comparison of running times on F_1 (PS = order of the partial sum).

Error tolerance	DSUAFD(PS)	UAFD(PS)	AFD(PS)	FD(PS)
0.5×10^{0}	8.379 s(1)	8.281 s(1)	0.2083 s(1)	0.6537 s(9)
0.5×10^{-1}	15.37 s(3)	15.68 s(3)	0.7291 s(4)	0.5679 s(20)
0.5×10^{-2}	18.90 s(4)	18.99 s(4)	1.174 s(7)	1.110 s(32)
0.5×10^{-3}	25.85 s(6)	25.55 s(6)	1.959 s(12)	1.690 s(43)
0.5×10^{-4}	29.80 s(7)	29.25 s(7)	2.744 s(22)	2.423 s(55)

6.2. Experiment 2

In this experiment, a ladder signal is used to demonstrate the effectiveness of the proposed method. The original signal is

$$F_2(t) = \begin{cases} 2, & 0.375\pi < t \le 0.625\pi, \\ 5, & 0.625\pi < t \le 1.25\pi, \\ 3, & 1.25\pi < t \le 1.75\pi, \\ 1, & \text{otherwise}, \end{cases} \tag{18}$$

where $t \in [0, 2\pi]$.

Figs. 7–11 show the real parts of the original signal and of the partial sums corresponding to the four algorithms. Tables 4 and 5 illustrate the relative energy errors and pointwise errors. In addition, we give the error curves of the four algorithms in Fig. 12. Table 6 shows the respective computer running times. These experimental results demonstrate the effectiveness of the newly proposed adaptive mono-component decompositions. Note that DSUAFD performs comparably with UAFD in this experiment. They both perform better than AFD and FD on F_2. We can reconstruct the signal by using a smaller number of iterations in DSUAFD and UAFD.
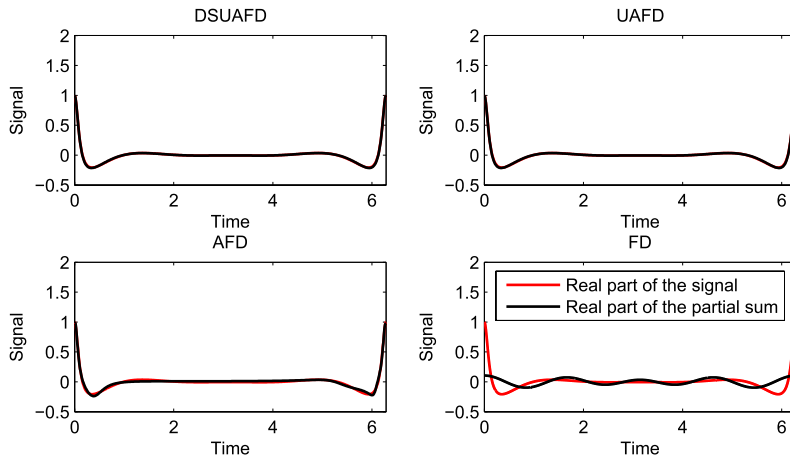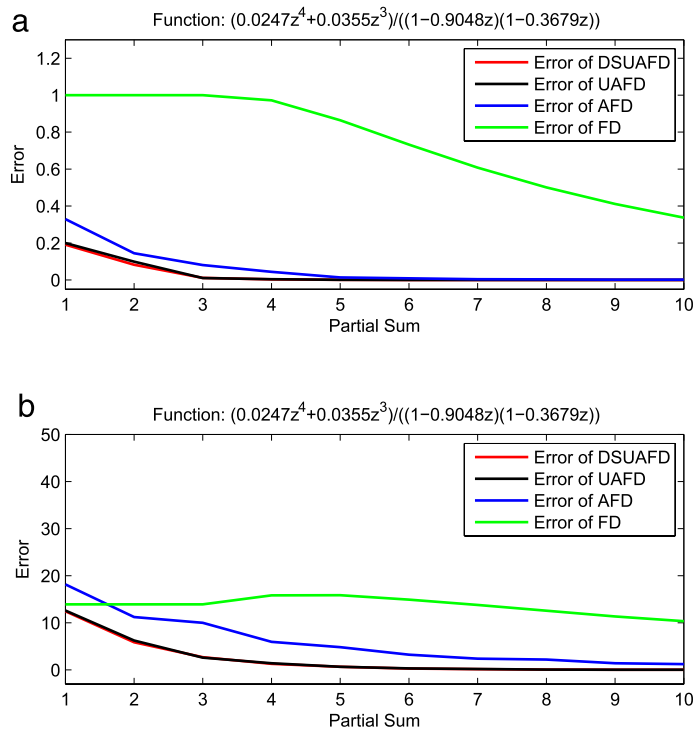
Fig. 5. The 5th partial sums of F_1.

Fig. 6. (a) Relative energy error curves and (b) pointwise error curves of F_1.

Table 4
Relative energy errors of F_2.

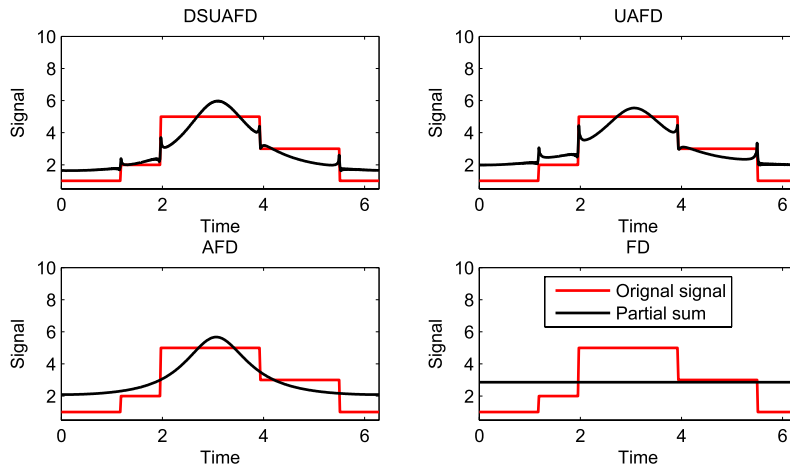| Partial sum	DSUAFD	UAFD	AFD	FD
1	0.5230×10^{-1}	0.5605×10^{-1}	0.7470×10^{-1}	0.2400
2	0.1003×10^{-1}	0.1081×10^{-1}	0.4370×10^{-1}	0.3896×10^{-1}
3	0.3431×10^{-2}	0.3176×10^{-2}	0.1601×10^{-1}	0.2728×10^{-1}
4	0.3164×10^{-3}	0.4236×10^{-3}	0.1104×10^{-1}	0.2476×10^{-1}
5	0.9346×10^{-4}	0.2123×10^{-3}	0.8722×10^{-2}	0.1887×10^{-1}
6	0.2156×10^{-4}	0.1800×10^{-3}	0.5832×10^{-2}	0.1482×10^{-1}
7	0.2902×10^{-5}	0.1591×10^{-3}	0.4724×10^{-2}	0.1352×10^{-1}
8	0.1021×10^{-5}	0.1541×10^{-3}	0.3237×10^{-2}	0.1341×10^{-1}
9	0.2909×10^{-6}	0.1537×10^{-3}	0.2449×10^{-2}	0.8791×10^{-2}
10	0.3000×10^{-7}	0.1535×10^{-3}	0.2044×10^{-2}	0.8754×10^{-2}

Fig. 7. The 1st partial sums of F_2.
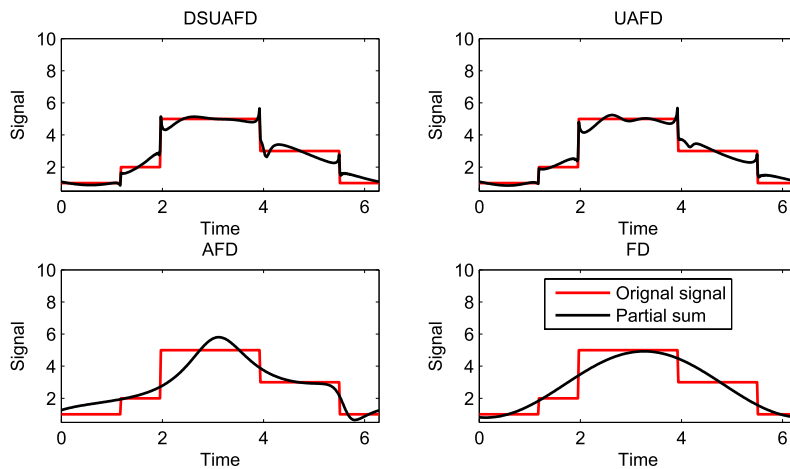
Fig. 8. The 2nd partial sums of F_2.

Table 5
Pointwise errors of F_2.

Partial sum	DSUAFD	UAFD	AFD	FD
1	0.2575×10^3	0.2758×10^3	0.3191×10^3	0.5570×10^3
2	0.9815×10^2	0.1054×10^3	0.2038×10^3	0.1982×10^3
3	0.5242×10^2	0.5414×10^2	0.1278×10^3	0.1702×10^3
4	0.1771×10^2	0.2098×10^2	0.1105×10^3	0.1588×10^3
5	0.8863×10^1	0.1422×10^2	0.8972×10^2	0.1222×10^3
6	0.4283×10^1	0.1306×10^2	0.6930×10^2	0.1104×10^3
7	0.1613×10^1	0.1289×10^2	0.5233×10^2	0.1091×10^3
8	0.8819×10^1	0.1276×10^2	0.4884×10^2	0.1092×10^3
9	0.5038	0.1278×10^2	0.3893×10^2	0.7951×10^2
10	0.1571	0.1277×10^2	0.3671×10^2	0.7859×10^2

6.3. Experiment 3

The original signal is

$$F_3 = \frac{(1 + 2z^2)}{(z - 2)(z - 3)} - \frac{1}{(z + 2)(z + 3)} e^{\frac{z+1}{z-1} + \frac{z+i}{z-i} + \frac{z-i}{z+i}}, \tag{19}$$

where $z \in \mathcal{C}$. The signal involves a singular inner function part induced by a singular measure consisting of three Dirac type point measures at, respectively, 1, i, and $-i$. In our experiment, the values of the signal at singular points are determined by their nearby points.
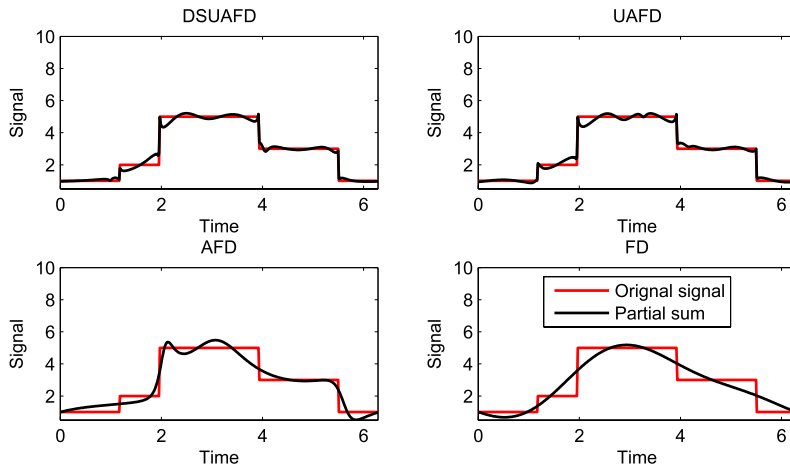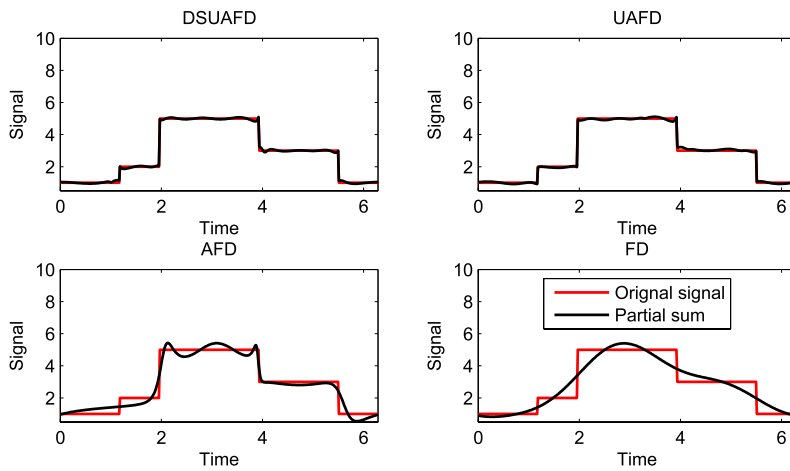
Fig. 9. The 3rd partial sums of F_2.
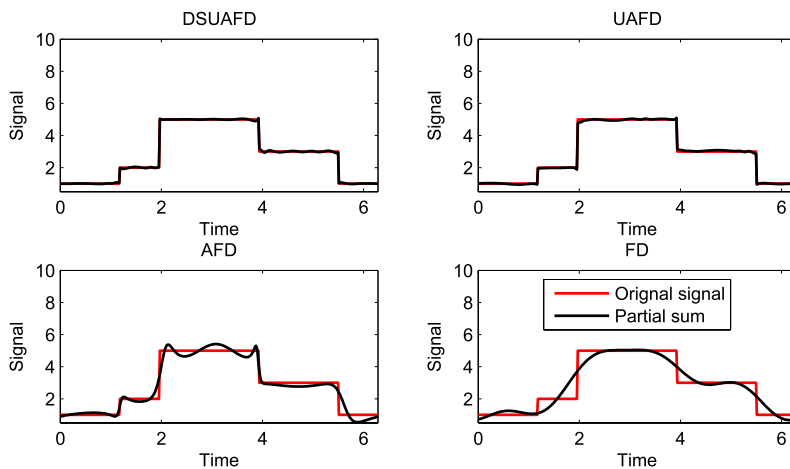

Fig. 10. The 4th partial sums of F_2.

Fig. 11. The 5th partial sums of F_2.

This signal is more complex than the signals in the previous two experiments. Figs. 13–17 show the real parts of the original signal and of the partial sums corresponding to the four algorithms. Tables 7 and 8 illustrate the relative energy errors and pointwise errors. In addition, we also give the error curves of the four algorithms in Fig. 18. In Table 9, we give the
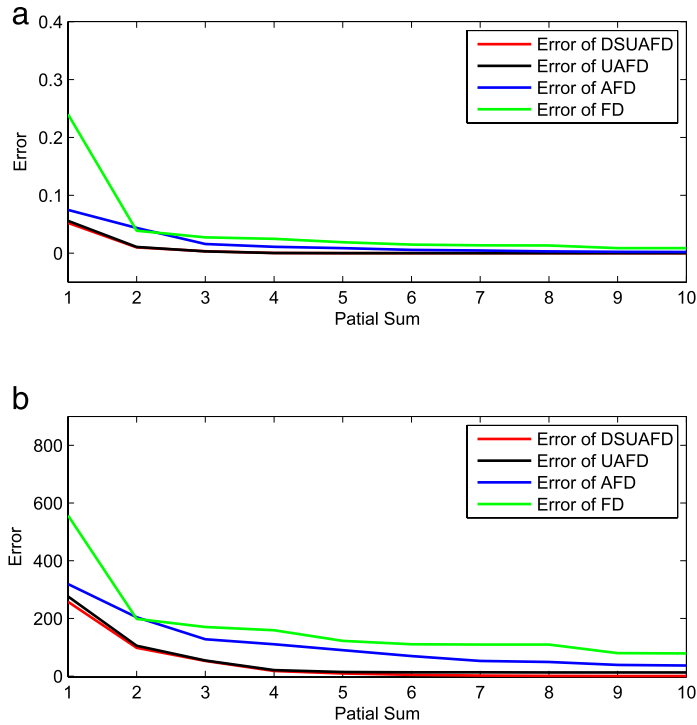
Fig. 12. (a) Relative energy error curves and (b) pointwise error curves of F_2.
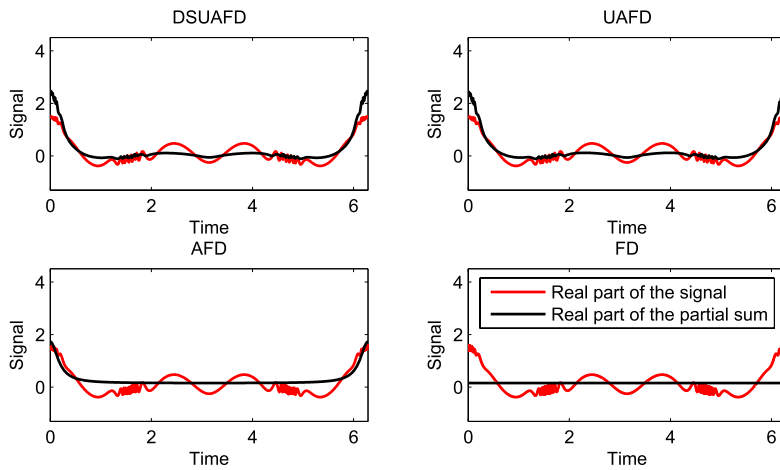

Fig. 13. The 1st partial sums of F_3.

Table 6
Comparison of running times on F_2 (PS = degree of the partial sum).

Error tolerance	DSUAFD(PS)	UAFD(PS)	AFD(PS)	FD(PS)
0.5×10^{0}	9.084 s(1)	9.217 s(1)	8.868 s(1)	0.01248 s(1)
0.5×10^{-1}	12.50 s(2)	12.52 s(2)	9.189 s(2)	0.01358 s(2)
0.5×10^{-2}	15.85 s(3)	15.83 s(3)	11.04 s(7)	0.02420 s(19)
0.5×10^{-3}	19.27 s(4)	19.12 s(4)	15.89 s(20)	N/A
0.5×10^{-4}	25.97 s(6)	N/A	21.17 s(33)	N/A

comparison of the respective computer running times. These experimental results demonstrate the effectiveness of DSUAFD and UAFD. In this experiment neither AFD, nor FD gives effective approximation to F_3.
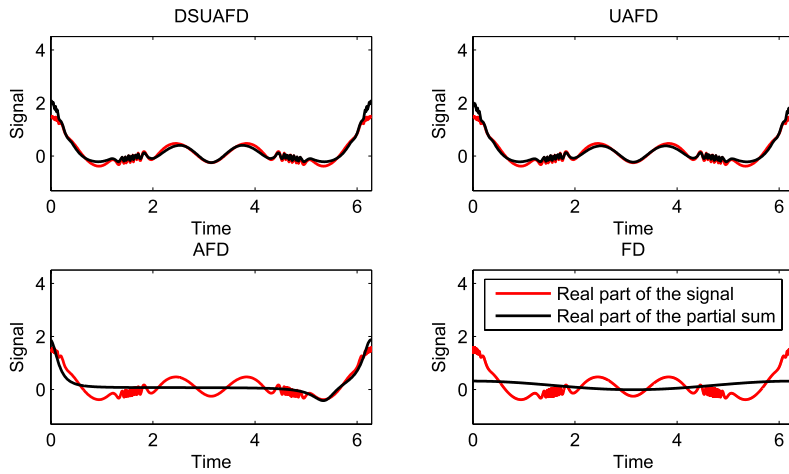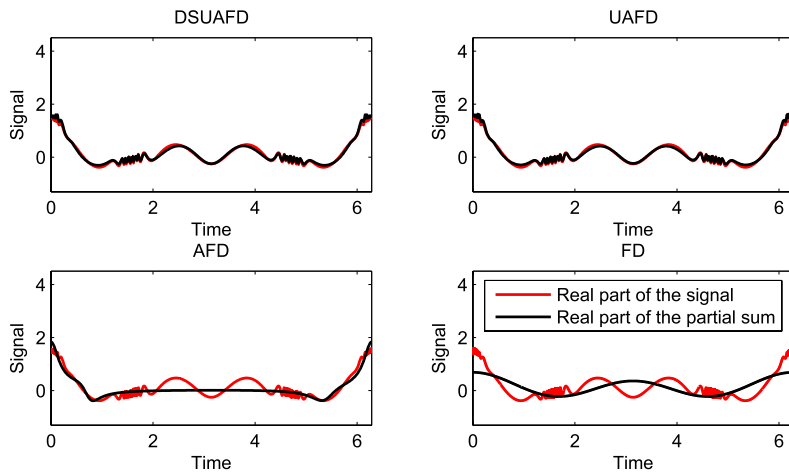
Fig. 14. The 2nd partial sums of F_3.

Fig. 15. The 3rd partial sums of F_3.

Table 7
Relative energy errors of F_3.

Partial sum	DSUAFD	UAFD	AFD	FD
1	0.2546	0.2439	0.3865	0.9437
2	0.8269×10^{-1}	0.7640×10^{-1}	0.2627	0.8846
3	0.1220×10^{-1}	0.1241×10^{-1}	0.1880	0.5777
4	0.3315×10^{-2}	0.3410×10^{-2}	0.1254	0.1675
5	0.1899×10^{-3}	0.7231×10^{-3}	0.7631×10^{-1}	0.1484
6	0.7031×10^{-3}	0.1856×10^{-3}	0.5805×10^{-1}	0.2737×10^{-1}
7	0.5253×10^{-4}	0.4459×10^{-4}	0.4186×10^{-1}	0.2533×10^{-1}
8	0.1406×10^{-4}	0.1097×10^{-4}	0.3423×10^{-1}	0.2291×10^{-1}
9	0.4278×10^{-5}	0.2779×10^{-5}	0.2633×10^{-1}	0.2201×10^{-1}
10	0.1126×10^{-5}	0.6655×10^{-6}	0.2112×10^{-1}	0.2155×10^{-1}

6.4. Experiment 4

The original signal is

$$F_3 = \left[\frac{(1 + 2z^2)}{(z-2)(z-3)} - \frac{1}{(z+2)(z+3)} \right] e^{\frac{z+1}{z-1} + \frac{z+i}{z-i} + \frac{z-i}{z+i}}, \tag{20}$$

where $z \in \mathcal{C}$. This signal has a singular inner function factor having three singular points at 1, i, and $-i$.

Figs. 19–23 show the real parts of the original signal and those of the partial sums corresponding to the four algorithms. Tables 10 and 11 illustrate the relative energy errors and pointwise errors. We give the error curves of the four algorithms
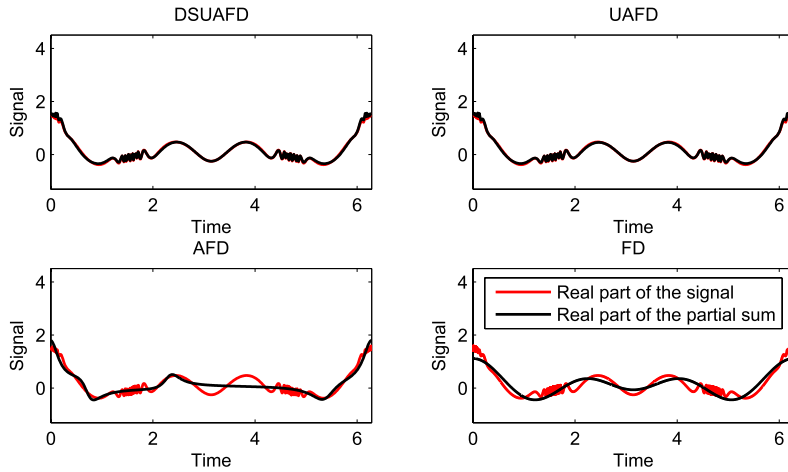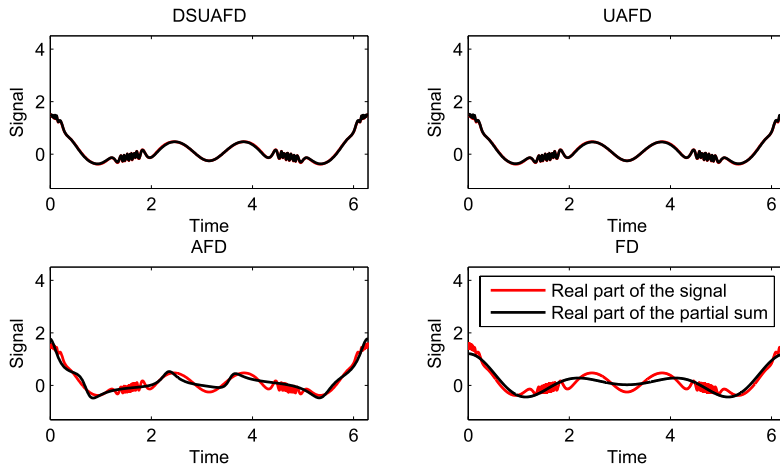
Fig. 16. The 4th partial sums of F_3.

Fig. 17. The 5th partial sums of F_3.

Table 8
Pointwise errors of F_3.

Partial sum	DSUAFD	UAFD	AFD	FD
1	0.5867×10^2	0.5765×10^2	0.8078×10^2	0.1114×10^3
2	0.2871×10^2	0.2847×10^2	0.6322×10^2	0.1136×10^3
3	0.1309×10^2	0.1313×10^2	0.5176×10^2	0.9532×10^2
4	0.6168×10^1	0.6361×10^1	0.4167×10^2	0.5262×10^2
5	0.3058×10^1	0.3148×10^1	0.3483×10^2	0.4999×10^2
6	0.1478×10^1	0.1814×10^1	0.2990×10^2	0.1800×10^2
7	0.7962	0.7741	0.2534×10^2	0.1568×10^2
8	0.3800	0.3689	0.2253×10^2	0.1696×10^2
9	0.2148	0.1916	0.1941×10^2	0.1602×10^2
10	0.1018	0.9073×10^{-1}	0.1758×10^2	0.1635×10^2

Table 9
Comparison of running times on F_3 (PS = order of the partial sum).

Error tolerance	DSUAFD(PS)	UAFD(PS)	AFD(PS)	FD(PS)
0.5×10^0	8.641 s(1)	8.982 s(1)	0.4963 s(1)	1.140 s(4)
0.5×10^{-1}	15.87 s(3)	15.93 s(3)	1.582 s(7)	1.574 s(6)
0.5×10^{-2}	19.91 s(4)	19.90 s(4)	37.05 s(39)	51.55 s(96)
0.5×10^{-3}	27.80 s(6)	27.39 s(6)	N/A	N/A
0.5×10^{-4}	33.99 s(8)	31.15 s(7)	N/A	N/A

a Function: $(1+2z^2)/((z-2)(z-3))-(1/(z+2)(z+3))\exp((z+1)/(z-1)+(z+i)/(z-i)+(z-i)/(z+i));$

b Function: $(1+2z^2)/((z-2)(z-3))-1/(z+2)(z+3)\exp((z+1)/(z-1)+(z+i)/(z-i)+(z-i)/(z+i))$
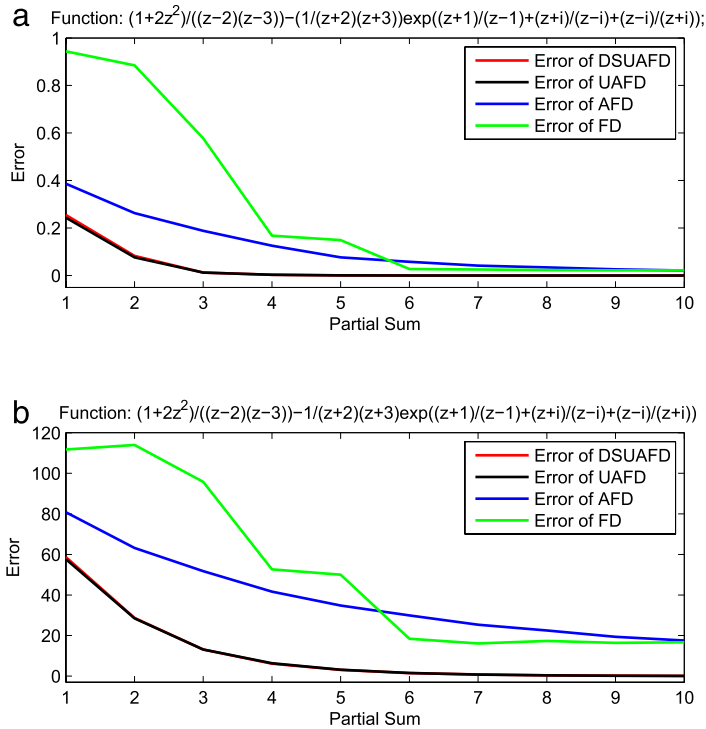

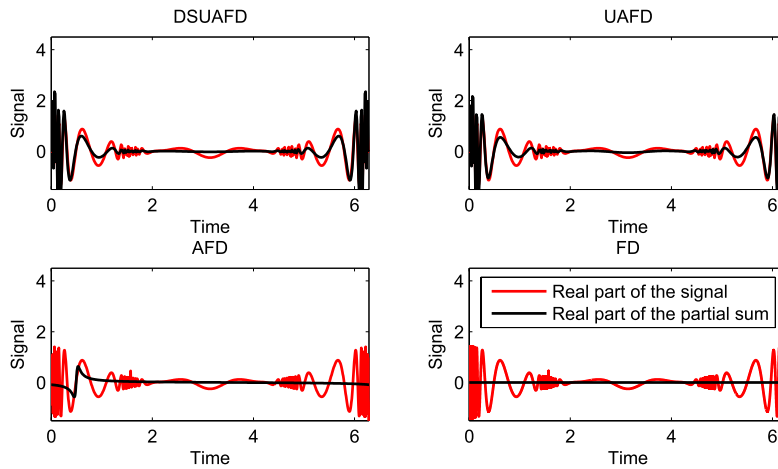**Fig. 18.** (a) Relative energy error curves and (b) pointwise error curves of F_3.

Fig. 19. The 1st partial sums of F_4.

in Fig. 24. The comparison of the computer running times is presented in Table 12. These experimental results demonstrate the effectiveness of DSUAFD and UAFD in this experiment. It seems that AFD and FD do not provide effective approximation to singular inner functions.

6.5. Experiment 5

In this experiment we produce mono-component-based time–frequency distributions (MTFDs) of the functions F_1 and F_2. Figs. 25 and 26 show MTFDs of F_1 and F_2.

6.6. Discussions and Conclusions

The four mono-component decomposition models, of which three are adaptive, are extensively compared. In terms of iteration times, the three adaptive mono-component decompositions are more effective than the traditional Fourier series.
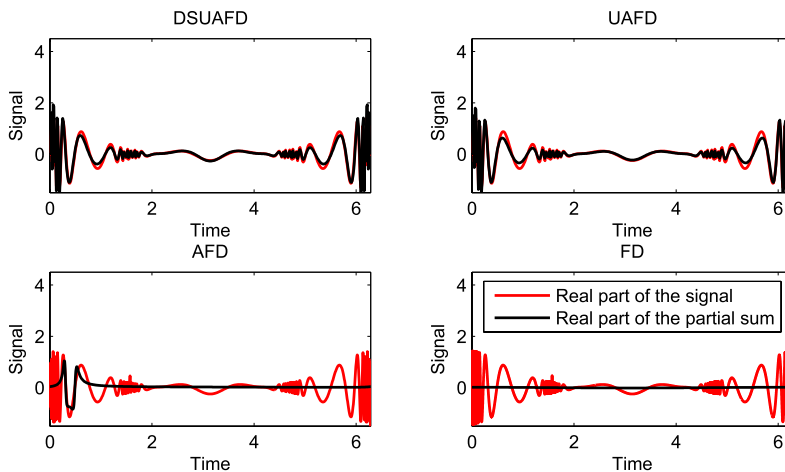
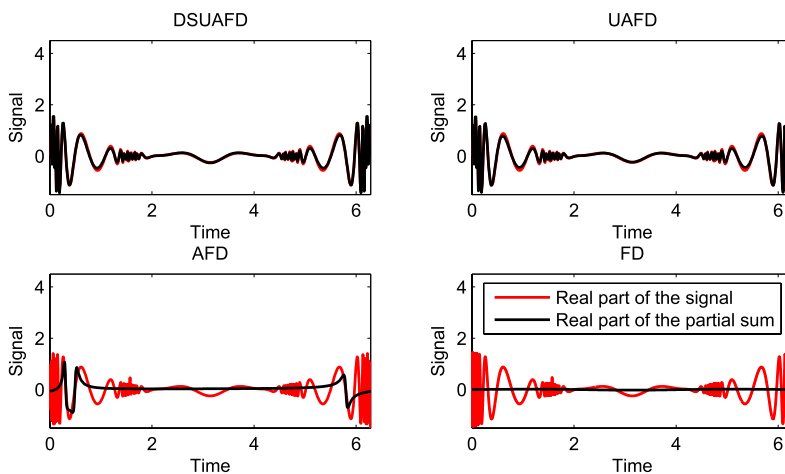**Fig. 20.** The 2nd partial sums of F_4.

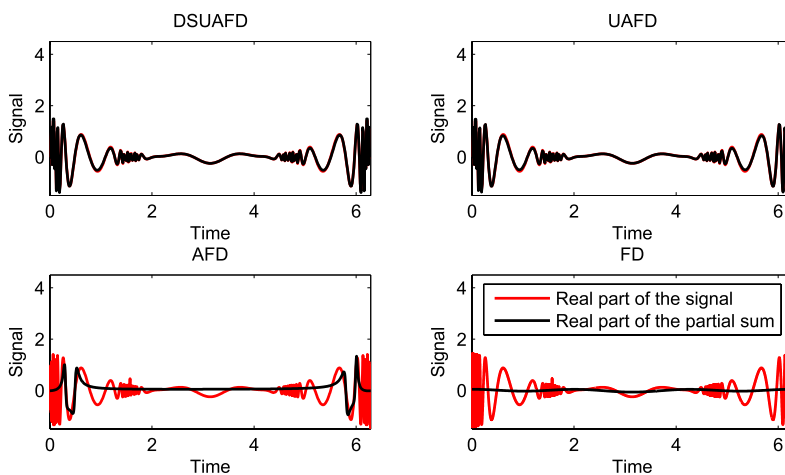**Fig. 21.** The 3rd partial sums of F_4.

Fig. 22. The 4th partial sums of F_4.

The DSUAFD and UAFD models are superb. For singular inner functions AFD and FD almost have no effect, while DSUAFD and UAFD can do effective approximation. Among DSUAFD and UAFD the latter is more preferable, for, to gain a similar accuracy, UAFD has a less complicated algorithm and requires less computer running time. In terms of computer running
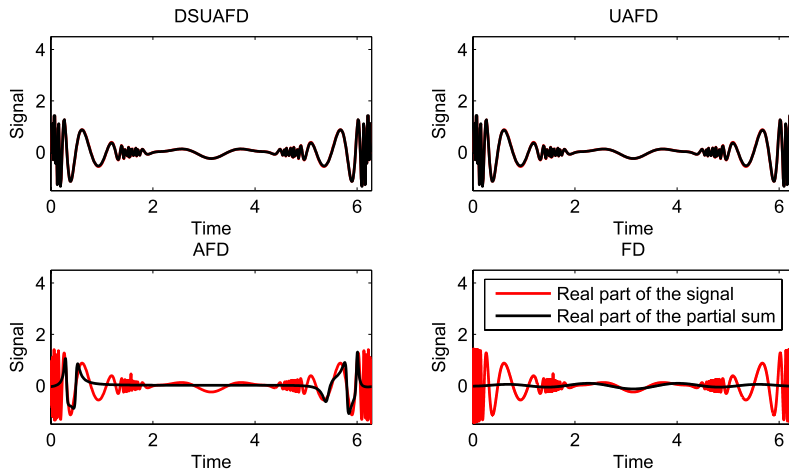
Fig. 23. The 5th partial sums of F_4.

Table 10
Relative energy errors of F_4.

Partial sum	DSUAFD	UAFD	AFD	FD
1	0.2443	0.1968	0.9279	0.1000×10^1
2	0.8113×10^{-1}	0.7023×10^{-1}	0.8453	0.9995
3	0.1131×10^{-1}	0.1230×10^{-1}	0.7588	0.9992
4	0.3390×10^{-2}	0.3473×10^{-2}	0.6755	0.9948
5	0.7033×10^{-3}	0.8315×10^{-3}	0.6118	0.9841
6	0.1942×10^{-3}	0.2059×10^{-3}	0.5659	0.9840
7	0.5207×10^{-4}	0.5537×10^{-4}	0.5276	0.9557
8	0.1307×10^{-4}	0.1267×10^{-4}	0.4810	0.9550
9	0.4024×10^{-5}	0.3595×10^{-5}	0.4448	0.9532
10	0.9307×10^{-6}	0.7824×10^{-6}	0.4202	0.9083

Table 11
Pointwise errors of F_4.

Partial sum	DSUAFD	UAFD	AFD	FD
1	0.4801×10^2	0.4484×10^2	0.9040×10^2	0.9173×10^2
2	0.2344×10^2	0.2357×10^2	0.8617×10^2	0.9192×10^2
3	0.1052×10^2	0.1088×10^2	0.8154×10^2	0.9201×10^2
4	0.5233×10^1	0.5409×10^1	0.7781×10^2	0.9095×10^2
5	0.2549×10^1	0.2743×10^1	0.7182×10^2	0.8898×10^2
6	0.1266×10^1	0.1312×10^1	0.6982×10^2	0.8856×10^2
7	0.6609	0.6938	0.6818×10^2	0.8194×10^2
8	0.3199	0.3232	0.6420×10^2	0.8198×10^2
9	0.1757	0.1744	0.6282×10^2	0.8394×10^2
10	0.8247×10^{-1}	0.7976×10^{-1}	0.6209×10^2	0.8459×10^2

Table 12
Comparison of running times on F_4 (PS = order of the partial sum).

Error tolerance	DSUAFD(PS)	UAFD(PS)	AFD(PS)	FD(PS)
0.5×10^0	9.036 s(1)	8.467 s(1)	1.623 s(8)	7.140 s(25)
0.5×10^{-1}	16.46 s(3)	15.55 s(3)	N/A	N/A
0.5×10^{-2}	19.46 s(4)	19.59 s(4)	N/A	N/A
0.5×10^{-3}	27.57 s(6)	26.10 s(6)	N/A	N/A
0.5×10^{-4}	33.28 s(8)	33.76 s(8)	N/A	N/A

time, it is no wonder that DSUAFD and UAFD require considerably longer times, for they involve the factorization process. The compensation is that only a few terms can effectively reconstruct the given signal. It is remarkable that AFD is more effective than FD but requires not substantially more computer time. In fact, AFD gives rise to a practical algorithm of best approximation by rational functions of degrees less than n. We will treat this issue in a separate paper.
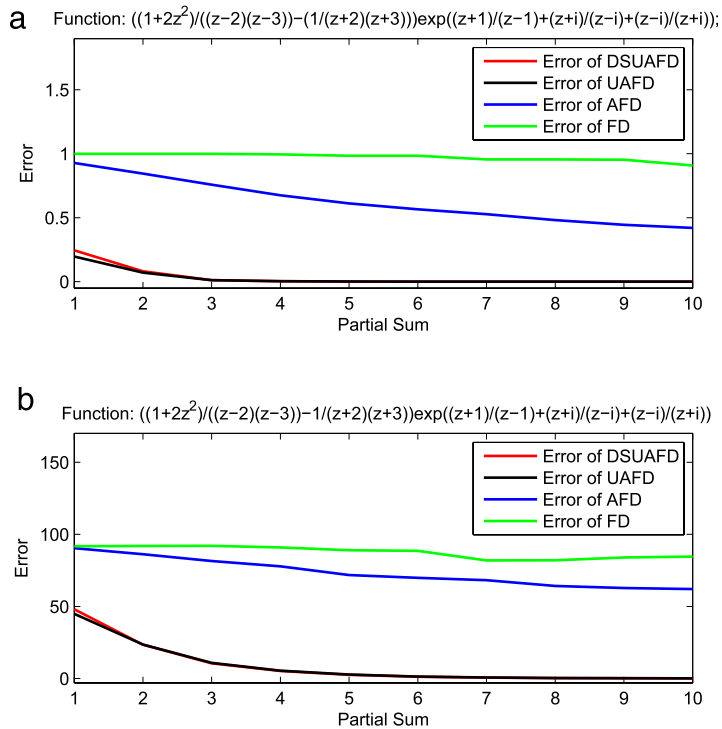
a   Function: $((1+2z^2)/((z-2)(z-3))-(1/(z+2)(z+3)))\exp((z+1)/(z-1)+(z+i)/(z-i)+(z-i)/(z+i));$

b   Function: $((1+2z^2)/((z-2)(z-3))-1/(z+2)(z+3))\exp((z+1)/(z-1)+(z+i)/(z-i)+(z-i)/(z+i))$

Fig. 24. (a) Relative energy error curves and (b) pointwise error curves of F_4.
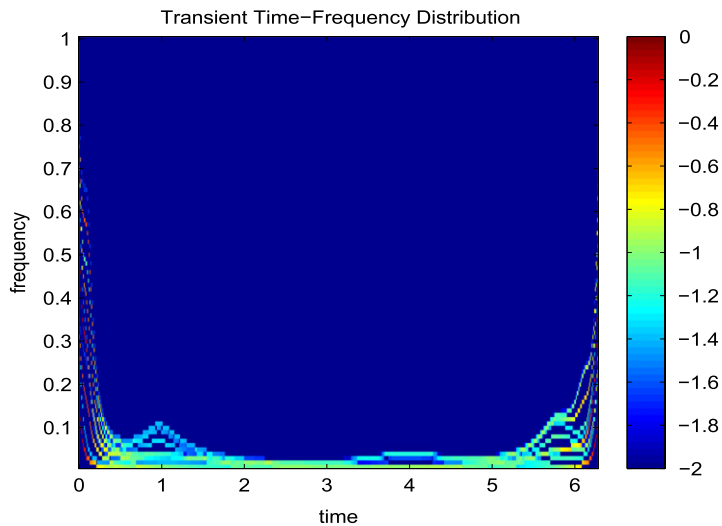
Fig. 25. MTFD of F_1.

Acknowledgments
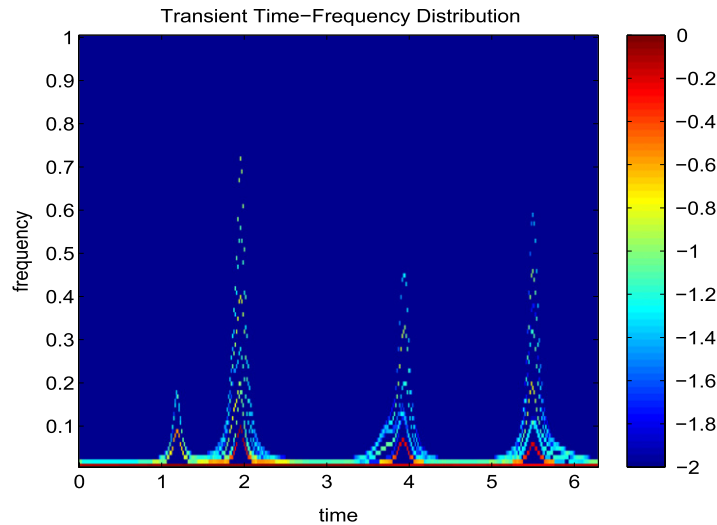
Fig. 26. MTFD of F_2.

References

 [1] T. Qian, Analytic signals and harmonic measures, Journal of Mathematical Analysis and Applications 314 (2006) 526–536.
 [2] T. Qian, Mono-components for decomposition of signals, Mathematical Methods in the Applied Sciences 29 (2006) 1187–1198.
 [3] T. Qian, Q.H. Chen, L.Q. Li, Analytic unit quadrature signals with non-linear phase, Physica D: Nonlinear Phenomena 303 (2005) 80–87.
 [4] Y.X. Fu, L.Q. Li, Generalized analytic signal associated with linear canonical transform, Optics Communications 281 (2008) 1468–1472.
 [5] Y.X. Fu, L.Q. Li, Nontrivial harmonic waves with positive instantaneous frequency, Nonlinear Analysis 68 (2008) 2431–2444.
 [6] P. Dang, T. Qian, Analytic phase derivative, all-pass filters and signals of minimum phase, IEEE Transactions on Signal Processing 59 (2011) 4708–4718.
 [7] T. Qian, Boundary derivatives of the phases of inner and outer functions and applications, Mathematical Methods in the Applied Sciences 32 (2009) 253–263.
 [8] L.H. Tan, L.X. Shen, L.H. Yang, Rational orthogonal bases satisfying the Bedrosian identity, Advances in Computational Mathematics 33 (2010) 285–303.
 [9] B. Yu, H. Zhang, The Bedrosian identity and homogeneous semi-convolution equations, Journal of Integral Equations and Applications 20 (2008) 527–568.
[10] E. Bedrosian, A product theorem for Hilbert transform, Proceedings of the IEEE 51 (1963) 868–869.
[11] T. Qian, Intrinsic mono-component decomposition of functions: an advance of Fourier theory, by T. Qian, Mathematical Methods in the Applied Sciences 33 (2010) 880–891.
[12] T. Qian, Y. Wang, Adaptive Fourier series-a variation of greedy algorithm, Advances in Computational Mathematics 34 (2011) 279–293.
[13] T. Qian, L. Tan, Y. Wang, Adaptive decomposition by weighted inner functions, The Journal of Fourier Analysis and Applications 17 (2011) 175–190.
[14] Q.H. Chen, L.Q. Li, T. Qian, Two families of unit analytic signals with nonlinear phase, Physica D 221 (2006) 1–12.
[15] R.A. Devore, V.N. Temlyakov, Some remarks on greedy algorithm, Advances in Computational Mathematics 5 (1996) 173–187.
[16] H. Akcay, On the uniform approximation of discrete-time systems by generalized Fourier series, IEEE Transactions on Signal Processing 49 (2011) 1461–1467.
[17] R. Bojanic, An estimate of the rate of convergence of Fourier series of functions of bounded variation, Publications de l'Institut Mathématique 26 (1979) 57–60.
[18] V.V. Savchuk, Best linear methods for approximation of bounded harmonic functions, Nonlinear Oscillations 2 (2008) 255–264.
[19] L.H. Tan, C.Y. Zhou, The point-wise convergence of general rational Fourier series, Mathematical Methods in the Applied Sciences. http://dx.doi.org/10.1002/mma.2636.
[20] H. Akcay, B. Niness, Orthonormal basis functions for modelling continuous-time systems, Signal Processing 77 (1999) 261–274.
[21] A. Bultheel, P. Gonz alez-Vera, E. Hendriksen, O. Njastad, Orthogonal Rational Functions, in: Cambridge Monographs on Applied and Computational Mathematics, vol. 5, Cambridge University Press, 1999.
[22] A. Bultheel, P. Carrette, Takenaka–Malmquist basis and general Toeplitz matrices, in: Proceedings of the 42nd CDC Conference, Maui, Hawaii, vol. 1, 2003, pp. 486–491.
[23] A. Bultheel, P. Carrette, Fourier analysis and the Takenaka–Malmquist basis, in: Conference on Decision and Control Maui, Hawaii, USA, December 1, 2003, pp. 486–491.
[24] B. Ninness, H. Hjalmarsson, F. Gustafsson, Generalized Fourier and Toeplitz results for rational orthonormal bases, SIAM Journal on Control and Optimization 37 (1999) 429–460.
[25] J.L. Walsh, Interpolation and Approximation by Rational Functions in the Complex Plane, American Mathematical Society, Providence, Rhode Island, 1969.
[26] M. Pap, Hyperbolic wavelets and multiresolution in $H^2(T)$, The Journal of Fourier Analysis and Applications 17 (2011) 755–776.
[27] W. Mi, T. Qian, Frequency domain identification: an algorithm based on adaptive rational orthogonal system, Automatica 48 (2012) 1154–1162.
[28] W. Mi, T. Qian, F. Wan, A fast adaptive model reduction method based on Takenaka–Malmquist systems, Systems and Control Letters 61 (2012) 223–230.
[29] T. Qian, The optimal approximation by n-Blaschke forms, Preprint.
[30] H. Li, L.Q. Li, T. Qian, Discrete-time analytic signals and Bedrosian product theorems, Digital Signal Processing 20 (2010) 982–990.
[31] H. Li, L.Q. Li, Y.Y. Tang, Mono-component decomposition of signals based on Blaschke basis, International Journal of Wavelets, Multiresolution and Information Processing 5 (2007) 941–956.
[32] L. Cohen, Time–Frequency Analysis: Theory and Applications, Prentice Hall, 1995.
[33] G. Davis, S. Mallat, M. Avellaneda, Adaptive greedy approxiamtions, Constructive Approximation 13 (1997) 57–98.
[34] V.N. Temlyakov, The best m-term approximation and greedy algorithm, Advances in Computational Mathematics 8 (1998) 249–265.
[35] T. Qian, Liming Zhang, Zhi-Xiong Li, Algorithm of adaptive Fourier decomposition, IEEE Transactions on Signal Processing 59 (2011) 5899–5906.
[36] Q.S. Cheng, Digital Signal Processing, Peking University Press, 2003.
[37] J.B. Garnett, Bounded Analytic Functions, Academic Press, 1987.